Phys. Status Solidi A, nº 9, 2161-2165 (2009)

Structural and photoluminescence studies of erbium implanted nanocrystalline silicon thin films

M.F. Cerqueira[*1], P. Alpuim[1], S.A. Filonovich[1], E. Alves[2], A.G. Rolo[1], G. Andres[1], J. Soares[3] and A. Kozanecki[4]

[1] Departamento de Física, Universidade do Minho, Campus de Azurém, 4800-058 Guimarães, Portugal
[2] Instituto Tecnológico e Nuclear, EN 10, 2686-953 Sacavém, Portugal
[3] Departamento de Física, Universidade de Aveiro, Campus de Santiago, 3700 Aveiro, Portugal
[4] Polish Academy of Sciences, Institute of Physics, PL-02668, Warsaw, Poland

Received ……., revised …….., accepted ……
Published online ……..

PACS 81.15.Gh, 81.07.Bc, 78.67.Bf, 78.30._j, 81.40.Ef

*Corresponding author: e-mail fcerqueira@fisica.uminho.pt, Phone: +253 60 4332, Fax: +253 678981

Hydrogenated amorphous and nanocrystalline silicon thin films deposited by Hot Wire (HW) and Radio-Frequency Plasma-Enhanced (RF) Chemical Vapor Deposition were Erbium-implanted. Their pre-implantation structural properties and post-implantation optical properties were studied and correlated. After one-hour annealing at 150ºC in nitrogen atmosphere only amorphous films showed photoluminescence (PL) activity at 1.54 μm, measured at 5 K. After further annealing at 300ºC for one hour, all the samples exhibited a sharp PL peak positioned at 1.54 μm, with a FWHM of ~5 nm. Amorphous films deposited by HW originated a stronger PL peak than corresponding films deposited by RF, while in nanocrystalline films PL emission was much stronger in samples deposited by RF than by HW.
There was no noticeable difference in Er^{3+} PL activity between films implanted with $1x10^{14}$ atoms/cm^2 and $5x10^{15}$ atoms/cm^2 Er doses.

1 Introduction

A large improvement in light emission efficiency from Si-based materials is required if fully integrated silicon optoelectronics is to become a reality in the near future. Rare-earth doping of silicon has consistently attracted scientific interest as a strategy to achieve this goal, together with the exploitation of quantum confinement in silicon nanocrystals. Erbium-doping of Si is of special importance for optical communications due to the emission line at 1.54 μm. However, Er-doped bulk crystalline silicon still present unsolved problems, such as the strong temperature quenching of the Er emission [1]. A recent approach to the problem of light emission from silicon is the use of Si-nanocrystals, embedded in a matrix made of another Si-based material, as sensitizers for Er [2-5]. It has been shown [3,6] that the effective Er^{3+} excitation cross section increases by more than two orders of magnitude when Si-nanocrystals are added to the SiO_x matrix.
In this paper, we used an hydrogenated amorphous silicon matrix where the Si nanocrystals are embedded , followed by an Er-implantation step to achieve Er-doped hydrogeneted nanocrystalline silicon (nc-Si:Er:H). Hydrogenated amorphous silicon films deposited in the same reactor were also Er-implanted (a-Si:Er:H) and studied in parallel, for comparison. Low annealing temperatures (≤300ºC) in the post-implantation step were used for dopant activation and implantation-damage recovery. This annealing temperature range was chosen because in hydrogenated silicon films atomic hydrogen starts evolving from the silicon network at temperatures close to 400ºC, leaving behind many dan-

gling bonds and other structural defects. These defects, in turn, will act as non-radiative recombination centres that will hinder energy transfer to the emitting centre.

2 Experimental

Hydrogenated amorphous and nanocrystalline silicon films were deposited by Hot Wire Chemical Vapor Deposition (HW) and Radio-Frequency Plasma-Enhanced Chemical Vapor Deposition (RF) in a UHV system with a base pressure $\leq 2\times10^{-7}$ Torr, on double-polished crystalline silicon substrates. During deposition, substrates were heated up to a temperature of T_{sub}=150ºC or T_{sub}=220ºC. For the HW-CVD samples, a single tungsten filament of 0.5 mm diameter and approximately 14 cm length, bent to a coil and placed 4 cm from the substrate, was resistively heated with an AC power supply. The filament temperature of 1950°C was measured by a two-colour digital ratio pyrometer and the pressure during deposition was kept constant at 20 mTorr. For the RF samples, the inter-electrode distance was 3 cm, the density of power was 175 mW/cm^2 and the pressure was 150 mTorr. For both methods the silane flux, F_{SiH4} was kept at 1 sccm and the hydrogen flux, F_{H2}, was varied in order to obtain the desired dilution, defined as $D_H = F_{H2} / (F_{H2} + F_{SiH4})x100\%$. Details of the deposition process are given elsewhere [7].

Amorphous silicon (a-Si:H) films were deposited from pure silane and nc-Si:H films were deposited using D_H= 96% and 99% for HW and RF depositions, respectively.

Crystalline fraction, X_C, was estimated from Raman spectroscopy [8]. Dark conductivity was measured on aluminium (Al) parallel contacts between room temperature and 100ºC, before Er implantation.

Each as-deposited sample was divided into two pieces that were Er-implanted using two different beam fluences: 1x10^{14} atoms/cm^2 and 5x10^{15} atoms/cm^2. The depth profile was the same in both groups of samples and was centered at ~50 nm.

Rutherford Back -scattering spectroscopy (RBS) and Elastic Recoil Detection (ERD) were used for chemical composition and thickness evaluation. Photoluminescence (PL) measurements in the infrared region were performed with a Fourier-transform spectrometer. The signal was detected by a germanium detector and optical pumping was achieved using the 514.5 nm line of an Ar+ laser. Laser power was 200 mW and measurement temperature was 5K. PL measurements were performed after implantation and after each one-hour annealing treatment at 150ºC and 300ºC.

3 Results and discussion

From the structural point of view the as-deposited samples can be grouped, following their Raman spectra, in amorphous (S36 and S37) and nanocrystalline (S28 and S35). Figure 1 shows a typical Raman curve for each group. The broad band around 480 cm^{-1} is related to the amorphous silicon matrix and is present in all the samples. The presence of Si nanocrystals is visible in the Raman spectra by the relatively narrow peak in the vicinity of 520 cm^{-1}. This asymmetric peak is related to the transverse-longitudinal optical (TO-LO) confined phonon modes of nanocrystalline silicon.

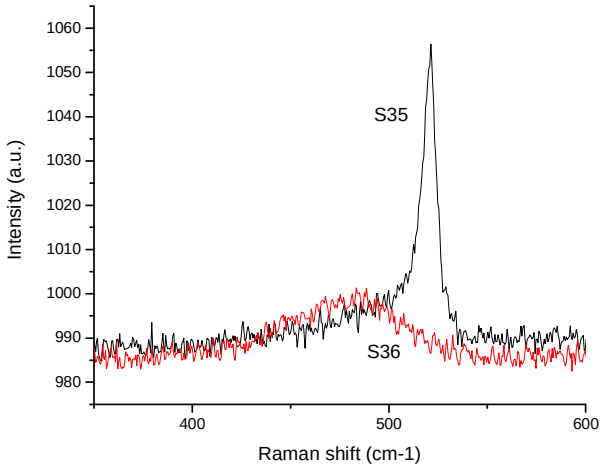

Figure 1 Raman spectra of one nanocrystalline-Si sample (S35) and of one amorphous-Si sample (S36).

The relative weight of the amorphous and crystalline bands in the Raman spectra is commonly used in order to estimate the volume fraction of the crystalline phase, X_C, through the following phenomenological relation [9 - 11]:

$$X_C = Ic/(Ic+yIa)$$

where Ic and Ia are the integrated intensities of the bands produced by the crystalline and amorphous phases, respectively, and y is an empirical parameter of the order of unity. Although the values of y that have been used for mixed-phase silicon vary considerably, the most recent data indicate that $1< y <2$ [10, 11]. We used y=1.7 [11]. The crystalline fraction obtained was X_C=47% and X_C=63% for samples S28 and S35, respectively.

The values of dark conductivity (σ_d), that can be seen in Table I, correlate well with the structural characteristics of the films: nanocrystalline samples have conductivities ~5 orders of magnitude higher than the amorphous samples, that have $\sigma_d = 2.5\times10^{-12}$ Ω^{-1}cm^{-1} and 5.5×10^{-10} Ω^{-1}cm^{-1} for the RF and HW samples, respectively. The oxygen measured by RBS, if present, was in all the samples lower than the resolution limit of the setup (<4 atom%).

Figure 2 shows the near-infrared photoluminescence spectra (IR PL-spectra) of nanocrystalline films after erbium implantation in the as- implanted state and before annealing. It can be seen that none of the samples shows the Er^{3+} characteristic emission at 1.54 μm. However, the spectra have a very intense and narrow (FWHM ~1.5 nm) peak at approximately 1.57 μm. Since this peak was not found in amorphous samples (not shown) it must be concluded that

it is the result of interactions between Er-ions and Si-nanocrystals.

Table I Composition, structural and electronic characteristics of the as-grown samples. C_H is the hydrogen content by ERD.

Sample	CVD	D_H (%)	T_{sub} (ºC)	C_H, at% (ERD)	% X_C (Raman)	σ_d^* ($\Omega^{-1}cm^{-1}$)
S28	RF	99	150	13-16	47	2.7×10^{-7}
S37	RF	0	240	18-23	0	2.5×10^{-12}
S35	HW	96	220	6-10	63	9.3×10^{-5}
S36	HW	0	220	15-20	0	5.5×10^{-10}

* dark conductivity was measured on similar samples deposited on polyimide

In general, the intensity of this peak (1.57 μm) decreases as the 1.54 μm peak increases with the annealing treatment [see Fig.3 (a)]. It may be interesting to note that this peak, which only appears in the nanocrystalline samples, is stronger in HW-as-implanted samples than in RF-ones (see Figure 2). However, in HW samples it quickly disappears upon annealing and in RF-samples the peak first increases upon annealing at 150ºC, disappearing only after annealing at higher temperature [see Fig.3 (a)].

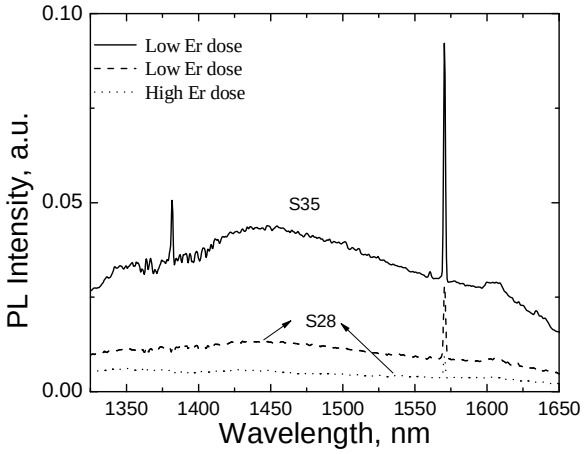

Figure 2 PL spectra measured at 5K of nanocrystalline-Si samples after Er implantation.

Figure 3 shows the photoluminescence spectra of the films after annealing at 150ºC (inset) and 300ºC, for nanocrystalline [Fig.3 (a)] and amorphous [Fig.3 (b)] samples. The spectra of all the samples after annealing at 300ºC are characterized by a peak around 1.54 μm which is the signature of the Er^{3+} emission centres. However, in nc-Si:Er:H films [Fig.3 (a)] this peak only appears after annealing at 300ºC. In contrast, a-Si:Er:H films [Fig.3 (b)] exhibit a small 1.54 μm emission peak immediately after the annealing step at 150ºC. No difference in the intensity of the 1.54 μm Er^{3+} peak can be noticed between low- and high-implanted-dose samples.

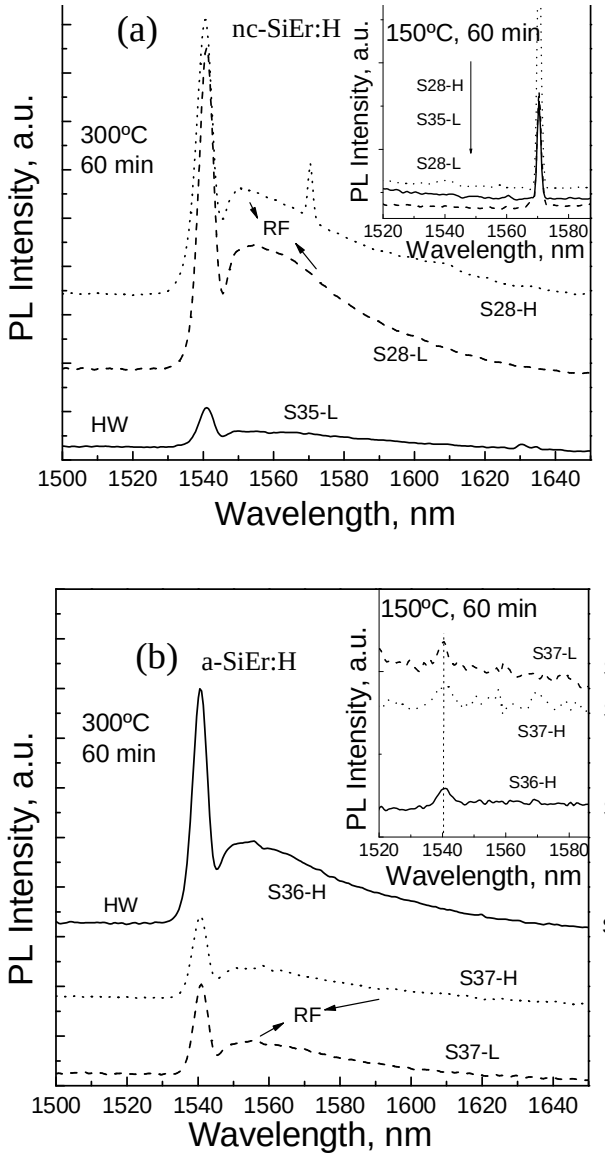

Figure 3 PL spectra measured at 5K of (a) nc-Si:Er:H films annealed at 300ºC for 1 hour, (b) a-Si:Er:H films annealed at 300ºC for 1 hour. Insets show PL spectra of same samples after 150ºC annealing for 1 hour. H and L refers to films implanted with 10^{15} Er atoms/cm^2 (high Er dose) and with $5x10^{14}$ atoms/cm^2 (low Er dose) respectively.

In all samples, the Er^{3+} PL intensity increases by several orders of magnitude after the annealing treatment at 300ºC. Since annealing at 300ºC cannot induce crystallization, the most important effect here should be the reduction of the

number of defects (their passivation with hydrogen) and implantation-damage recovery. Consequently a reduction of the number of non-radiative pathways for recombination of electron-hole pairs occurs with annealing and so the Er^{3+} PL increases. This process of network local reconstruction can also lead to the activation of the charge-transfer dopants since it is assisted by mobile light atoms (e.g. hydrogen or oxygen) in the Si network. There is evidence that maximal PL intensity from Er^{3+} in silicon is mediated by oxygen [12, 13], with the formation of ErO_3 clusters which show acceptor-like behaviour. Optimal oxygen content for this process is 10 oxygen atoms per Er atom which under the implantation doses used is still below the detection edge of the RBS technique.

Comparing the Er^{3+} PL intensity for samples deposited by HW and by RF it can be seen that nc-Si:Er:H films [Fig.3 (a)] deposited by HW produce a much weaker Er^{3+} PL peak than corresponding films deposited by RF, while the opposite is true for a-Si:Er:H films [Fig.3 (b)], where PL emission is much stronger in samples deposited by HW than in those deposited by RF.

Whichever the interaction mechanism present (dipole-dipole interaction or direct electron exchange), the energy transfer to the Er^{3+} ions could be mediated by the amorphous silicon matrix or by the Si nanocrystals.

Since we have observed that i) the sample with the highest crystalline fraction before implantation results in the implanted one with the weakest Er^{3+} PL-emission; ii) the erbium PL emission from amorphous and from nanocrystalline samples is similar; and iii) the amorphous samples show a clear Er^{3+}-PL peak already when annealed at temperatures as low as 150ºC, it seems plausible that in all samples the energy transfer to Er^{3+} ions is mediated by the a-Si:H matrix and not by the Si nanocrystals.

Furthermore, the crystalline volume fraction of nc-Si:H films deposited by RF (47%) and by HW (63%) %) anti-correlates with the (higher) Er^{3+} PL peak in the RF samples when compared with the corresponding (lower) peak in the HW samples, after 300ºC annealing.

Nevertheless more experiments are required, namely it is necessary to continue to anneal until higher temperatures (at least 800ºC), keeping track of any structural changes that might occur in the films after each annealing step, and correlate them with the measured PL spectrum. This will be the next step of this work.

More insight into the PL features was gained analyzing the temperature effect on the Er emission. Figure 4 shows the Er^{3+} photoluminescence as a function of temperature. The intensity of the erbium emission strongly decreases with increasing temperature (for temperatures higher than 250K), giving information that thermal quenching mechanisms of the Er PL are active.

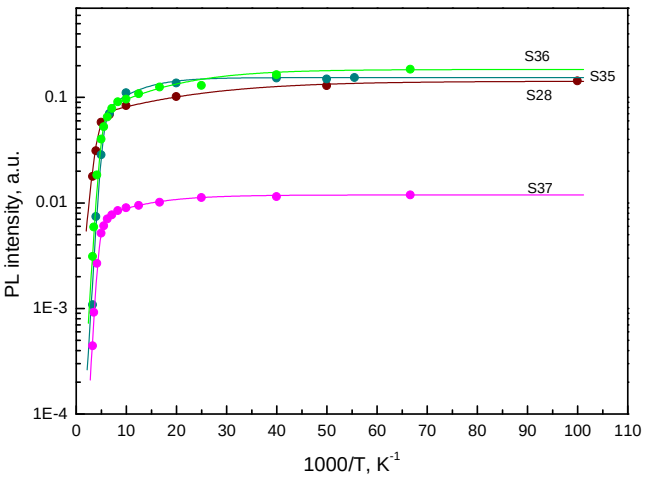

Figure 4 Er^{3+} photoluminescence intensity as a function of temperature.

The PL temperature dependance was analyzed using the following fit function, which assumes a characteristic thermally activated excitation process, according to [14]:

$$I(T) = I(0)\left[1 + C_1 \exp\left(-E_1 / kT\right) + C_2 \exp\left(-E_2 / kT\right)\right]^{-1}$$

where E_1 is the activation energy for the high temperature range and E_2 is the corresponding energy for the low temperature region. The coefficients C_1 and C_2 take into account the excitation processes of Er ions.

The percentage of Er PL at room temperature (RT) compared with the PL at 5 K is quite low, approximately 4% for sample S37, 2% for S36 and 1% for S35. These results also indicate that the Er^{3+} PL quenching is not related with microstructure but with hydrogen content (see Table I), since the PL quenching is more severe in samples containing less hydrogen. This decrease on the Er^{3+} PL quenching could be due to a more complete hydrogen passivation of defects (at grain boundary) that act as non-radiative recombination centers. It is well known that for the growth of good quality amorphous silicon thin films hydrogen is essential for improving their optical and electrical activity, since it will bind to silicon atoms saturating the silicon dangling bonds.

4 Conclusions

Hot-wire and RF-PECVD low-temperature deposition of silicon thin films with efficient light emission from implanted erbium ions at 5K was demonstrated. Er-ions are excited efficiently through energy transfer from the host after an annealing treatment at 300ºC for 1 hour. In the as-implanted samples there was no Er^{3+} emission due to implantation-damage. However, the as-implanted nc-Si:Er:H films show a sharp peak around 1.57 μm which decreases

and disappears as the Er-1.54 μm peak develops after each annealing step.
nc-Si:Er:H films deposited by RF have stronger PL-emission than those deposited by HW, while the opposite happens in a-Si:Er:H. No effect of Er implantation dose was detected in the emission spectrum within the range of implantation dose studied in this paper. Severe PL quenching was observed in all samples when measured at room temperature. PL temperature dependence study indicates that the hydrogen content plays an important role on the Er^{3+} PL quenching.

Acknowledgements One of the authors (S.A.F.) acknowledges FCT for a Post-doctorate grant (SFRH/BPD/14919/2004).

References

[1] M. Forcales, T. Gregorkiewicz and M. S. Bresler, Phys. Rev. B **68**, p. 035213 (2003).
[2] M. Fujii, M. Yoshida, Y. Kanzawa, S. Hayashi, K. Yamamoto, Appl. Phys. Lett. **71**, p. 1198 (1997).
[3] F. Priolo, G. Franzò, D. Pacifici, V. Vinciguerra, F. Iacona, A. Irrera, J. Appl. Phys. **89**, p. 264 (2001).
[4] C-C Kao, C. Barthou, B. Gallas, S. Fisson, G. Vuve, J. Rivory, A. Al Choueiry, A-M Jurdyc, B. Jacquier, L. Bigot, J. Appl. Phys. **98**, p. 013544 (2005).
[5] C. Oton, W.H. Loh, A.J. Kenyon, Appl. Phys. Lett. **89**, p. 031116 (2006).
[6] P. G. Kik, A. Polman, J. Appl. Phys. **88**, p. 1992 (2000).
[7] P. Alpuim, M. Ribeiro, S.A. Filonovich, Mater. Sci. Forum **514-16**, p. 475 (2006).
[8] T. Kaneko, M. Wakagi, K. Onisawa, T. Minemura, Appl. Phys. Lett. **64**, p. 1865 (1994).
[9] R. Tsu, J. Gonzalez-Hernandez, S. S. Chão, S. C. Lee and K. Tanaka, Appl. Phys. Lett. **40**, p. 534 (1982).
[10] M. Ledinsky, L. Fekete, J. Stuchlik, T. Mates, A. Fejfar and J. Koška, J. Non-Cryst. Solids **352**, p. 1209 (2006).
[11] E. Vallat-Sauvain, C. Droz, F. Mellaud, J. Bailat, A. Shah and C. Ballif, J. Non-Cryst. Solids **352,** p. 1200 (2006).
[12] L.R. Tessler, C. Piamontezem, M.C. Martins Alves, H. Tolentino, J. Non-Cryst. Solids **266-269**, p. 598 (2000).
[13] A. Kozanecki, D. Kuritsyn, H. Przybyliska, W. Jantsch, Physica B: Cond. Matter **308-310**, p. 354 (2001).
[14] H. Przybylinska, W. Jantsch, Yu. Suprun-Belevitch, M. Stepikhova, L. Palmetshofer, G. Hendorfer, A. Kozanecki, R. J. Wilson and B. J. Sealy, Phys. Rev. B 54, 2532 (1996)